

An Old Disk That Can Still Form a Planetary System

Edwin A. Bergin¹, L. Ilesedore Cleeves¹, Uma Gorti^{2,3}, Ke Zhang⁴, Geoffrey A. Blake⁵, Joel D. Green⁶, Sean M. Andrews⁷, Neal J. Evans II⁶, Thomas Henning⁸, Karin Öberg⁷, Klaus Pontoppidan⁹, Chunhua Qi⁷, Colette Salyk¹⁰, & Ewine F. van Dishoeck^{11,12}

¹*Department of Astronomy, University of Michigan, 500 Church St., Ann Arbor, MI 48109, USA*

²*SETI Institute, Mountain View, CA, USA*

³*NASA Ames Research Center, Moffett Field, CA, USA*

⁴*California Institute of Technology, Division of Physics, Mathematics & Astronomy, MS 150-21, Pasadena, CA 91125, USA*

⁵*California Institute of Technology, Division of Geological & Planetary Sciences, MS 150-21, Pasadena, CA 91125, USA*

⁶*Department of Astronomy, The University of Texas, 2515 Speedway, Stop C1402, Austin, TX 78712, USA*

⁷*Harvard-Smithsonian Center for Astrophysics, 60 Garden Street, Cambridge, MA 02138, USA*

⁸*Max Planck Institute for Astronomy, Königstuhl 17, 69117, Heidelberg, Germany*

⁹*Space Telescope Science Institute, 3700 San Martin Drive, Baltimore, MD 21218, USA*

¹⁰*National Optical Astronomy Observatory, 950 N. Cherry Ave., Tucson, AZ 85719, USA*

¹¹*Max Planck Institut für Extraterrestrische Physik, Giessenbachstrasse 1, 85748, Garching, Germany*

¹²*Leiden Observatory, Leiden University, PO Box 9513, 2300 RA, Leiden, The Netherlands*

From the masses of planets orbiting our Sun, and relative elemental abundances, it is estimated that at birth our Solar System required a minimum disk mass of $\sim 0.01 M_{\odot}$ within ~ 100 AU of the star¹⁻⁴. The main constituent, gaseous molecular hydrogen, does not emit from the disk mass reservoir⁵, so the most common measure of the disk mass is dust thermal emission and lines of gaseous carbon monoxide⁶. Carbon monoxide emission generally probes the disk surface, while the conversion from dust emission to gas mass requires knowl-

edge of the grain properties and gas-to-dust mass ratio, which likely differ from their interstellar values^{7,8}. Thus, mass estimates vary by orders of magnitude, as exemplified by the relatively old (3–10 Myr) star TW Hya^{9,10}, with estimates ranging from 0.0005 to 0.06 M_{\odot} ^{11–14}. Here we report the detection the fundamental rotational transition of hydrogen deuteride, HD, toward TW Hya. HD is a good tracer of disk gas because it follows the distribution of molecular hydrogen and its emission is sensitive to the total mass. The HD detection, combined with existing observations and detailed models, implies a disk mass $>0.05 M_{\odot}$, enough to form a planetary system like our own.

Commonly used tracers of protoplanetary disk masses are thermal emission from dust grains and rotational lines of carbon monoxide gas. Both methods, however, rely on unconstrained assumptions. The dust method has to assume a dust opacity per gram of dust, and grain growth can change this value dramatically¹⁵. The gas mass is then calculated by multiplying the dust mass by the gas-to-dust ratio, usually assumed to be ~ 100 from measurements of the interstellar medium¹⁶. The gas mass thus rests on a large and uncertain correction factor. The alternative is to use rotational CO lines as gas tracers, but these are optically thick, and therefore trace the disk surface temperature, as opposed to the midplane mass. The use of CO as a gas tracer then leads to large discrepancies between mass estimates for different models of TW Hydrae (from $5 \times 10^{-4} M_{\odot}$ to 0.06 M_{\odot}), even though each matches a similar set of observations^{13,14}.

Using the Herschel Space Observatory¹⁷ PACS Spectrometer¹⁸ we robustly detected (9σ) the lowest rotational transition, $J = 1 \rightarrow 0$, of hydrogen deuteride (HD) in the closest ($D \sim 55$ pc) and best studied circumstellar disk around TW Hydrae (Fig. 1). This star is older (3–10 Million years^{9,10,19}) than most stars with gas-rich circumstellar disks⁸. The abundance of deuterium atoms relative to hydrogen is well characterized via atomic electronic transitions to be $x_D = 1.5 \pm 0.1 \times 10^{-5}$ in objects that reside within ~ 100 pc of the Sun²⁰. Placing atoms into H_2 and HD, which is appropriate for much of the disk mass, provides an HD abundance relative to H_2 of $x_{HD} = 3.0 \times 10^{-5}$. We combine the HD data with existing molecular observations to set new constraints on the disk mass within 100 AU – the most fundamental quantity that determines whether planets

can form. The disk mass also governs the primary mode of giant planet formation, either through core accretion or gravitational instability²¹. In this context we do not know whether our own Solar System formed within a typical disk, as nearly half of current disk mass estimates fall below the minimum mass solar nebula⁸. Our current census of extra-solar planetary systems furthermore suggests that even larger disk masses are necessary to form many of the planetary systems seen^{22,23}.

With smaller rotational energy spacings and a weak electric dipole moment, HD $J = 1 \rightarrow 0$ is a million times more emissive than H₂ for a given gas mass at a gas temperature of $T_{gas} = 20$ K. The HD line flux (F_l) sets a lower limit to the H₂ gas mass at distance D (see Supplementary Information):

$$M_{gas\ disk} > 5.2 \times 10^{-5} \left(\frac{F_l}{6.3 \times 10^{-18} \text{ W m}^{-2}} \right) \left(\frac{3 \times 10^{-5}}{x_{HD}} \right) \left(\frac{D}{55 \text{ pc}} \right)^2 \exp \left(\frac{128.5 \text{ K}}{T_{gas}} \right) M_{\odot}. \quad (1)$$

If HD is optically thick or D is hidden in other molecules such as PAHs or molecular ices, the conversion from deuterium mass to hydrogen mass will be higher and thus the mass will be larger, hence the lower limit. The strong temperature dependence arises from the fractional population of the $J=1$ state which has a value of $f_{J=1} \sim 3 \exp(-128.5 \text{ K}/T_{gas})$ for $T_{gas} < 50$ K in thermal equilibrium. Due to the low fractional population in the $J=1$ state, HD does not emit appreciably from gas with $T \sim 10 - 15$ K, the estimated temperature in the outer disk mass reservoir ($R \gtrsim 20\text{--}40$ AU). The HD mass derived from Eqn. (1) provides an estimate of the mass in warm gas, and is therefore a lower limit to the total mass within 100 AU.

The only factor in Eqn. (1) that could lower the mass estimate is a higher T_{gas} . The upper limit on the $J = 2 \rightarrow 1$ transition of HD (Fig. 1) implies $T_{gas} < 80$ K in the emitting region. This T_{gas} estimate yields $M_{gas\ disk} > 2.2 \times 10^{-4} M_{\odot}$, but T_{gas} is unlikely to be this high for the bulk of the disk. CO rotational transitions are optically thick and the level populations are in equilibrium with T_{gas} , so they provide a measure of T_{gas} . ALMA observations of CO $J = 3 \rightarrow 2$ emission in a $1.7'' \times 1.5''$ beam (radius ~ 43 AU) (see Supplementary Information and Supplementary Figure

1) yield an average $T_{gas} = 29.7$ K within 43 AU, and $M_{gas\ disk} > 3.9 \times 10^{-3} M_{\odot}$. This value is still likely to be too low because the optically thick CO emission presumably probes material closer to the surface than HD, and this gas will be warmer than the HD line emitting region. Thus essentially all correction factors would push the mass higher than this conservative limit, which already rules out a portion of the low end of previous mass determinations.

To determine the mass more accurately, we turn to detailed models that incorporate explicit gas thermal physics providing for substantial radial and vertical thermal structure. Both published models of the TW Hya disk reproduce a range of gas phase emission lines, but in one case with $M_{gas-disk} = 0.06 M_{\odot}$ ¹⁴ and in the other with $M_{gas-disk} = 0.003 M_{\odot}$ ¹³ (see Supplementary Information and Supplementary Table S1). These models were both placed into detailed radiation transfer simulations. The results from this calculation and the adopted physical structure are given in Fig. 2 for the model with $M_{gas-disk} = 0.06 M_{\odot}$. Fig. 2c shows the cumulative flux as a function of radius for the higher mass model; over 80% of the emission is predicted to arise from gas inside of 80 AU. Furthermore Fig. 2d provides a calculation of the HD emissive mass as a function of gas temperature. This calculation suggests gas with temperatures of 30–50 K is responsible for the majority of the HD emission.

The model with $M_{gas-disk} = 0.003 M_{\odot}$ predicts an HD line flux of $F_l = 3.8 \times 10^{-19} \text{ W m}^{-2}$, more than an order of magnitude below the detected level. For this model to reach the observed flux the disk mass must be increased by a factor of 20, ruling out this low disk mass. The $M_{gas-disk} = 0.06 M_{\odot}$ model predicts $F_l = 3.1 \times 10^{-18} \text{ W m}^{-2}$, still a factor of two below the observed value. Even the “high” mass estimate is too low. Based on this model we estimate the disk gas mass within 80 AU, where the majority of HD emissions arise, is $0.056 M_{\odot}$. Both of these models match other observations as the low disk mass model matches CO and $^{13}\text{CO } J = 3 \rightarrow 2$, while the higher mass model reproduces CO $J = 2 \rightarrow 1$, $J = 3 \rightarrow 2$, $J = 6 \rightarrow 5$. Both compare emission predictions to other species as well. However, they differ by a factor of 10 in predicting the HD emission. This difference shows the value of HD in constraining masses.

The age of TW Hya is uncertain. The canonical age of the cluster is 10^{+10}_{-7} Million years⁹. However there could be an age spread in cluster members and ages estimated for TW Hya itself range from 3–10 Myr^{10,19}. Even at the low end of this range TW Hya is older than the half-life of gaseous disks, inferred to be about 2 Myr⁸. In the case of the TW Hya association there is also little evidence for an associated molecular cloud²⁴, which is an additional indicator that this system is *relatively* older than most gas-rich disks. The lifetime of the gaseous disk is important as it sets the available timeframe for the formation of gas giants equivalent to Jupiter or Saturn. Based on our analysis, TW Hya contains a massive gas disk ($\gtrsim 0.06 M_{\odot}$) that is several times the minimum mass required to make the planets in our solar system. Thus, this “old” disk can still form a planetary system like our own.

The recent detection of cold water vapor from TW Hya found indirect evidence for a large water ice reservoir (\sim several thousand Earth oceans) assuming a disk mass of $0.02 M_{\odot}$ ²⁵. Our higher mass estimate implies a larger water ice reservoir, perhaps increased by a factor of two. The mass estimate in this one system lies on the upper end of previous mass measurements⁸, hinting that other disk masses are underestimated. The main uncertainty in the masses derived here is the gas temperature structure of the disk. Looking forward, observations of optically thick molecular lines, particularly CO, can be used to trace the *thermal structure of gas* in the disk. Observations of rarer CO isotopologues then provide constraints on the temperature in deeper layers²⁶. With the Atacama Large Millimeter Array, we will readily resolve multiple gas temperature tracers inside 80 AU where HD strongly emits. When used in tandem with HD we will be able to derive the gas mass with much greater accuracy (our simulations suggest to within a factor of 2–3). Moreover, additional HD detections could be provided by Herschel and with higher spectral resolution by SOFIA GREAT under favorable atmospheric conditions. These data could be used alongside emission from species such as $C^{18}O$, $C^{17}O$, or the dust to calibrate these more widely available probes to determine the disk gas mass. Thus, with the use of HD to complement other observations and constrain models we may finally place useful constraints on one of the most important quantities that governs the process of planetary birth.

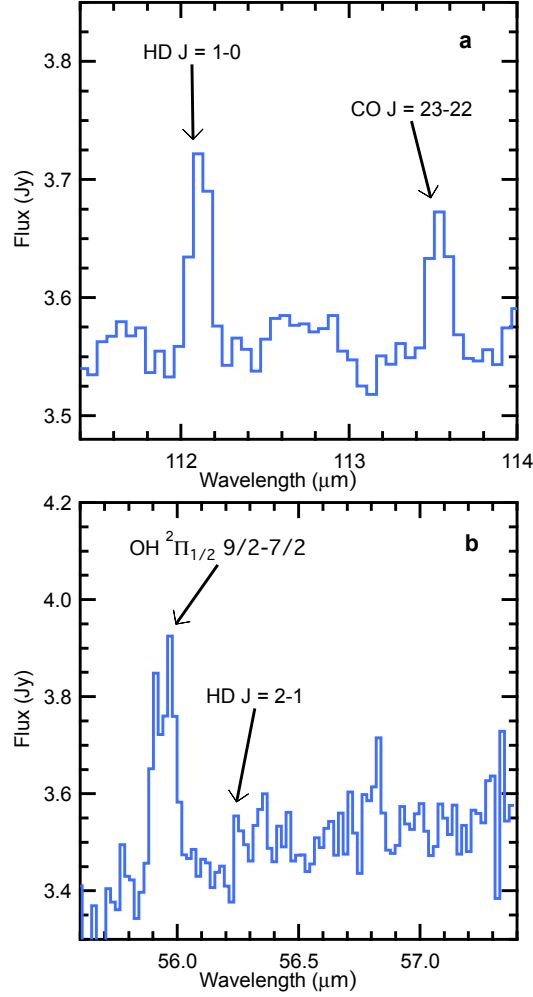


Figure 1: Herschel detection of Hydrogen Deuteride in the TW Hya protoplanetary disk. (a) The fundamental $J = 1 \rightarrow 0$ line of HD lies at $\sim 112\mu\text{m}$ line. On 20 November 2011 it was detected towards the TW Hya disk at the level of 9σ . The total integrated flux is $6.3 \pm 0.7 \times 10^{-18} \text{ W m}^{-2}$. We also report a detection of the warm disk atmosphere in CO $J = 23 \rightarrow 22$ with a total integrated flux of $4.4 \pm 0.7 \times 10^{-18} \text{ W m}^{-2}$. The $J = 1 \rightarrow 0$ line of HD was previously detected in a warm gas cloud exposed to radiation from nearby stars²⁷ by the Infrared Space Observatory. Other transitions have also been detected in shocked regions associated with supernova and outflows from massive stars^{28,29}. (b) Simultaneous observations of HD $J = 2 \rightarrow 1$ are shown. For HD $J = 2 \rightarrow 1$ we find a detection limit of $< 8.0 \times 10^{-18} \text{ W m}^{-2}$ (3σ). We also report a detection of the OH $^2\Pi_{1/2} \frac{9}{2} \rightarrow \frac{7}{2}$ doublet near $55.94 \mu\text{m}$ with an integrated flux of $4.93 \pm 0.27 \times 10^{-17} \text{ W m}^{-2}$. The spectra include the observed thermal dust continuum of $\sim 3.55 \text{ Jy}$ at both wavelengths.

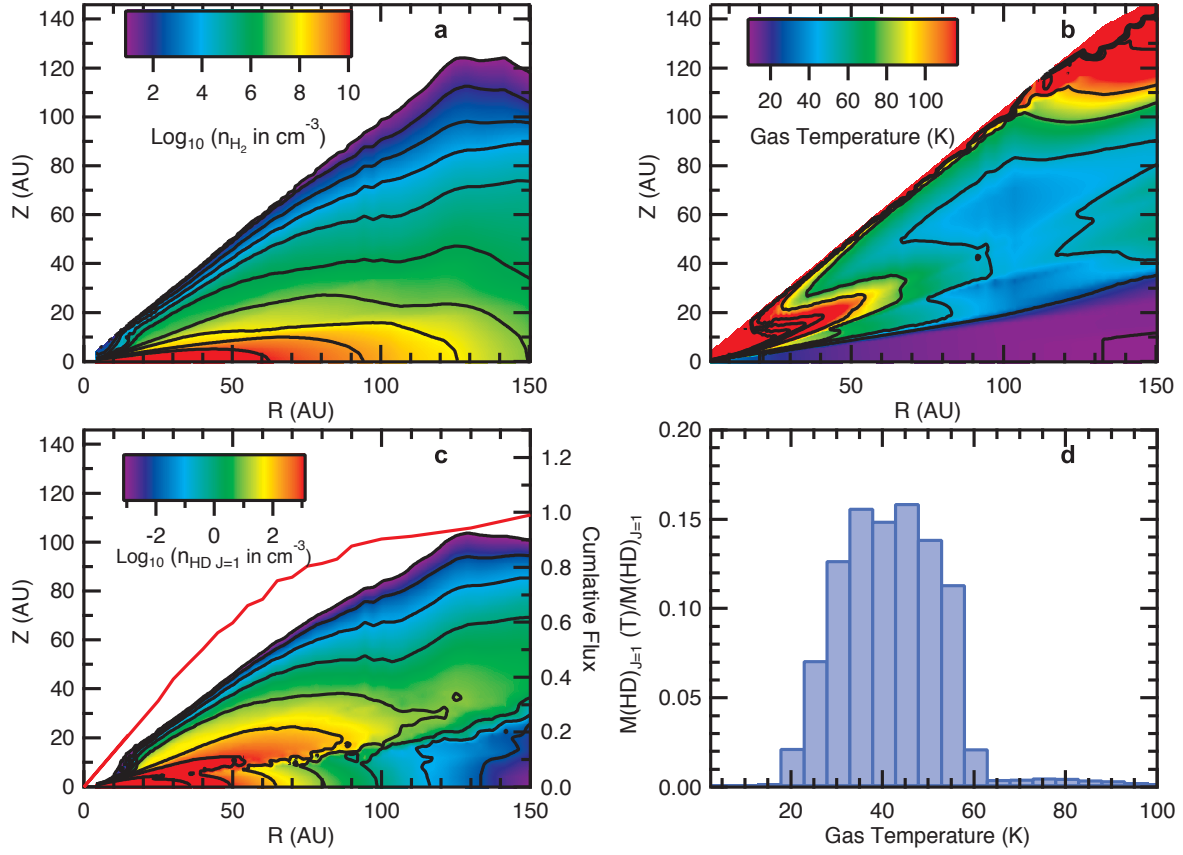


Figure 2: Model of the physical structure and HD emission in the TW Hya circumstellar disk.

(a) Radial and vertical distribution of the H_2 volume density, n_{H_2} , calculated in a model disk with mass $0.06 M_{\odot}$ ¹⁴. Contours start from the top at $\text{Log}_{10}[n_{\text{H}_2}/\text{cm}^{-3}] = 1.0$ and step downwards in units of factors of ten. (b) The gas temperature structure as derived by the thermochemical model¹⁴. Contours are 10, 25, 50, 75, 100, 150, 200, 250, and 300 K. (c) Radial and vertical distribution of the HD $J=1$ volume density, $n_{\text{HD } J=1}$, predicted in a model disk with the gas density and temperature structure as given in panels (a) and (b), with an HD abundance relative to H_2 of 3.0×10^{-5} . Contours start at the top with $\text{Log}_{10}[n_{\text{HD } J=1}/\text{cm}^{-3}] = -3$ and are stepped in factors of 10. The red line on the plot shows the cumulative flux contribution as a function of radius in terms of fractions of the overall predicted flux of $3.1 \times 10^{-18} \text{ W m}^{-2}$. To predict the HD line emission we calculate the solution of the equations of statistical equilibrium including the effects of line and dust opacity using the LIME code³⁰. (d) Fraction of the HD emission arising from gas with different temperatures, computed as function of the mass of HD excited to the $J=1$ state in gas at temperatures binned in units of 5 K and normalized to the total mass of HD in $J=1$. In particular, $\int n_{\text{HD } J=1} 2\pi R dr dz$ is computed successively in gas temperature bins of 5 K and then normalized to the total mass of HD in the $J=1$ state.

1. Kuiper, G. P. The Formation of the Planets, Part III. *Journal Royal Ast. Soc. of Canada* **50**, 158–176 (1956).
2. Kusaka, T., Nakano, T. & Hayashi, C. Growth of Solid Particles in the Primordial Solar Nebula. *Progress of Theoretical Physics* **44**, 1580–1595 (1970).
3. Weidenschilling, S. J. Aerodynamics of solid bodies in the solar nebula. *MNRAS* **180**, 57–70 (1977).
4. Hayashi, C. Structure of the Solar Nebula, Growth and Decay of Magnetic Fields and Effects of Magnetic and Turbulent Viscosities on the Nebula. *Progress of Theoretical Physics Supplement* **70**, 35–53 (1981).
5. Carmona, A. *et al.* A search for mid-infrared molecular hydrogen emission from protoplanetary disks. *Astron. & Astrophys.* **477**, 839–852 (2008).
6. Beckwith, S. V. W., Sargent, A. I., Chini, R. S. & Guesten, R. A survey for circumstellar disks around young stellar objects. *Astron. J.* **99**, 924–945 (1990).
7. Hartmann, L. Masses and mass distributions of protoplanetary disks. *Physica Scripta Volume T* **130**, 014012 (2008).
8. Williams, J. P. & Cieza, L. A. Protoplanetary Disks and Their Evolution. *Ann. Rev. Astron. Astrophys.* **49**, 67–117 (2011).
9. Barrado Y Navascués, D. On the age of the TW Hydrae association and 2M1207334-393254. *Astron. & Astrophys.* **459**, 511–518 (2006).
10. Vacca, W. D. & Sandell, G. Near-infrared Spectroscopy of TW Hya: A Revised Spectral Type and Comparison with Magnetospheric Accretion Models. *Astrophys. J.* **732**, 8 (2011).
11. Weintraub, D. A., Zuckerman, B. & Masson, C. R. Measurements of Keplerian rotation of the gas in the circumbinary disk around T Tauri. *Astrophys. J.* **344**, 915–924 (1989).
12. Calvet, N. *et al.* Evidence for a Developing Gap in a 10 Myr Old Protoplanetary Disk. *Astrophys. J.* **568**, 1008–1016 (2002).

13. Thi, W.-F. *et al.* Herschel-PACS observation of the 10 Myr old T Tauri disk TW Hya. Constraining the disk gas mass. *Astron. & Astrophys.* **518**, 647–651 (2010).
14. Gorti, U., Hollenbach, D., Najita, J. & Pascucci, I. Emission Lines from the Gas Disk around TW Hydra and the Origin of the Inner Hole. *Astrophys. J.* **735**, 90 (2011).
15. Natta, A. *et al.* Dust in Protoplanetary Disks: Properties and Evolution. *Protostars and Planets V* 767–781 (2007).
16. Draine, B. T. *et al.* Dust Masses, PAH Abundances, and Starlight Intensities in the SINGS Galaxy Sample. *Astrophys. J.* **663**, 866–894 (2007).
17. Pilbratt, G., Riedinger, J. R., Passvogel, T. *et al.* The Herschel Space Observatory. *Astron. & Astrophys.* **518**, 3–8 (2010).
18. Poglitsch, A., Waelkens, C., Geis, N. *et al.* The Photodetector Array Camera and Spectrometer (PACS) on the Herschel Space Observatory. *Astron. & Astrophys.* **518**, 9–20 (2010).
19. Hoff, W., Henning, T. & Pfau, W. The nature of isolated T Tauri stars. *Astron. & Astrophys.* **336**, 242–250 (1998).
20. Linsky, J. L. Deuterium Abundance in the Local ISM and Possible Spatial Variations. *Space Sci. Rev.* **84**, 285–296 (1998).
21. Lissauer, J. J. & Stevenson, D. J. Formation of Giant Planets. *Protostars and Planets V* 591–606 (2007).
22. Greaves, J. S. & Rice, W. K. M. Have protoplanetary discs formed planets? *MNRAS* **407**, 1981–1988 (2010).
23. Mordasini, C., Alibert, Y., Benz, W., Klahr, H. & Henning, T. Extrasolar planet population synthesis . IV. Correlations with disk metallicity, mass, and lifetime. *Astron. & Astrophys.* **541**, A97 (2012).

24. Tachihara, K., Neuhäuser, R. & Fukui, Y. Search for Remnant Clouds Associated with the TW Hya Association. *Pub. Astron. Soc. Japan* **61**, 585–591 (2009).
25. Hogerheijde, M. R., Bergin, E. A., Brinch, C. *et al.* Detection of the Water Reservoir in a Forming Planetary System. *Science* **334**, 338–340 (2011).
26. Dartois, E., Dutrey, A. & Guilloteau, S. Structure of the DM Tau Outer Disk: Probing the vertical kinetic temperature gradient. *Astron. & Astrophys.* **399**, 773–787 (2003).
27. Wright, C. M., van Dishoeck, E. F., Cox, P., Sidher, S. D. & Kessler, M. F. Infrared Space Observatory-Long Wavelength Spectrometer Detection of the 112 Micron HD $J = 1 - 0$ Line toward the Orion Bar. *Astrophys. J. Letters* **515**, L29–L33 (1999).
28. Bertoldi, F., Timmermann, R., Rosenthal, D., Drapatz, S. & Wright, C. M. Detection of HD in the Orion molecular outflow. *Astron. & Astrophys.* **346**, 267–277 (1999).
29. Neufeld, D. A. *et al.* Spitzer Observations of Hydrogen Deuteride. *Astrophys. J. Letters* **647**, L33–L36 (2006).
30. Brinch, C. & Hogerheijde, M. R. LIME - a flexible, non-LTE line excitation and radiation transfer method for millimeter and far-infrared wavelengths. *Astron. & Astrophys.* **523**, A25 (2010).
31. Ott, S. The Herschel Data Processing System – HIPE and Pipelines – Up and Running Since the Start of the Mission. In Mizumoto, Y., Morita, K.-I. & Ohishi, M. (eds.) *Astronomical Data Analysis Software and Systems XIX*, vol. 434 of *Astronomical Society of the Pacific Conference Series*, 139–142 (2010).
32. Müller, H. S. P., Schlöder, F., Stutzki, J. & Winnewisser, G. The Cologne Database for Molecular Spectroscopy, CDMS: a useful tool for astronomers and spectroscopists. *Journal of Molecular Structure* **742**, 215–227 (2005).
33. Pachucki, K. & Komasa, J. Electric dipole rovibrational transitions in the HD molecule. *Phys. Rev. A* **78**, 052503 (2008).

34. Kauffmann, J., Bertoldi, F., Bourke, T. L., Evans, N. J., II & Lee, C. W. MAMBO mapping of Spitzer c2d small clouds and cores. *Astron. & Astrophys.* **487**, 993–1017 (2008).
35. Qi, C. *et al.* CO J = 6-5 Observations of TW Hydrae with the Submillimeter Array. *Astrophys. J. Letters* **636**, L157–L160 (2006).
36. Dorschner, J., Begemann, B., Henning, T., Jaeger, C. & Mutschke, H. Steps toward interstellar silicate mineralogy. II. Study of Mg-Fe-silicate glasses of variable composition. *Astron. & Astrophys.* **300**, 503–520 (1995).
37. Dullemond, C. P. & Dominik, C. The effect of dust settling on the appearance of protoplanetary disks. *Astron. & Astrophys.* **421**, 1075–1086 (2004).
38. van Zadelhoff, G.-J., van Dishoeck, E. F., Thi, W.-F. & Blake, G. A. Submillimeter lines from circumstellar disks around pre-main sequence stars. *Astron. & Astrophys.* **377**, 566–580 (2001).
39. Flower, D. R., Le Bourlot, J., Pineau des Forêts, G. & Roueff, E. The cooling of astrophysical media by HD. *MNRAS* **314**, 753–758 (2000).
40. Flower, D. R. A quantum mechanical study of the rotational excitation of HD by ? *Journal of Physics B Atomic Molecular Physics* **32**, 1755–1767 (1999).
41. Pollack, J. B. *et al.* Composition and radiative properties of grains in molecular clouds and accretion disks. *Astrophys. J.* **421**, 615–639 (1994).

Acknowledgements Herschel is an ESA space observatory with science instruments provided by European-led Principal Investigator consortia and with important participation from NASA. Support for this work was provided by NASA through an award issued by JPL/Caltech and by the National Science Foundation under grant 1008800. This paper makes use of the following ALMA data: ADS/JAO.ALMA#2011.0.00001.SV. ALMA is a partnership of ESO (representing its member states), NSF (USA) and NINS (Japan), together with NRC (Canada) and NSC and ASIAA (Taiwan), in cooperation with the Republic of Chile. The Joint ALMA Observatory is operated by ESO, AUI/NRAO and NAOJ.

Author Contributions EAB, IC, UG, and KZ performed the detailed calculations used in the analysis. JG reduced the Herschel data. SA provided detailed disk physical models and UG provided thermochemical models, both developed specifically for TW Hya. EAB wrote the manuscript with revisions by NJE. All authors were participants in the discussion of results, determination of the conclusions, and revision of the manuscript.

Competing Interests The authors declare that they have no competing financial interests.

Correspondence Correspondence and requests for materials should be addressed to Edwin Bergin (email: ebergin@umich.edu).

Supplementary Information

1. Herschel Observations

TW Hya ($\alpha(2000) = 11^h01^m51.91^s$; $\delta(2000) = -34^\circ43'17.0''$) was observed as part of an open time Herschel Program (OT1_ebergin_4) using the PACS¹⁸ instrument on November 20, 2011. The PACS Range scan chop-nod mode was used. The background emission from the the telescope and sky was subtracted using two nod positions $1.5'$ distant from the source in each direction. The data cover a small spectral range ($111.2\text{--}114.2\ \mu\text{m}$ and $55.6\text{--}57.1\ \mu\text{m}$), with high sampling density (for a total of 81 steps). The first range includes HD $J = 1 \rightarrow 0$ and the second was designed to detect HD $J = 2 \rightarrow 1$. We used 12 repetitions to increase sensitivity for a deep scan, for a total integration time of 25124 seconds (36 repetitions) on TW Hya. The predicted line RMS was $0.62 \times 10^{-18}\ \text{W m}^{-2}$ and $2.65 \times 10^{-18}\ \text{W m}^{-2}$ at 112 and 56 μm , respectively.

The data were reduced using the Herschel Interactive Processing Environment (HIPE)³¹ v8.1 pipeline (calibration set 32). PACS is a 5×5 integral field unit spectrometer with a pixel size of $9.4'' \times 9.4''$; the source showed no sign of extended emission beyond the point spread function and was centered within 0.2 pixels (within $2''$) of the centerpoint in each case. We used the standard “calibration block” script to reduce the data for optimal signal-to-noise utilizing only the central pixel of the array, and then scaled this value to the spectra extracted from the central 3×3 pixels. We compared this to the PSF-corrected output from the pipeline, and the flux levels matched to within 10%. The PSF-corrected flux was 10% *higher* than the 3×3 extraction, which indicates an overcorrection and no sign of extended emission. Thus, we increased the flux measured from the central-spaxel-only spectrum by 10% to match that of the 3×3 extraction, yielding line

fluxes, $F_l = (4.4 \pm 0.7) \times 10^{-18} \text{ W m}^{-2}$ for CO $J = 23 \rightarrow 22$ (centered at $113.509 \mu\text{m}$ indicating a possible blend between CO at $113.46 \mu\text{m}$ and H₂O at $113.53 \mu\text{m}$), and $F_l = (6.3 \pm 0.7) \times 10^{-18} \text{ W m}^{-2}$ for HD $J = 1 \rightarrow 0$ (centered at $112.086 \mu\text{m}$). The line flux was obtained using a Gaussian fit. The continuum was determined by a first-order polynomial simultaneous fit in a fairly tight region around the line, avoiding the CO transition. The HD $J = 2 \rightarrow 1$ transition was not detected with a 3σ upper limit of $F_l < 8.0 \times 10^{-18} \text{ W m}^{-2}$. The lines are not resolved with $\lambda/\Delta\lambda \sim 1000$ at $112 \mu\text{m}$ and ~ 1500 at $56 \mu\text{m}$. The absolute uncertainty on flux calibration is potentially larger, with an important factor being the overall pointing and presence/absence of extended flux. Because TW Hya is a point source, the observations are well centered, and we included a PSF correction, the uncertainty in F_l is limited to 10-20%, negligible compared to other uncertainties.

From the CDMS database³², the $J = 1 \rightarrow 0$ line at 2674.986 GHz has $E_{J=1} = 128.5 \text{ K}$ with $A_{10} = 5.44 \times 10^{-8} \text{ s}^{-1}$. The $J = 2 \rightarrow 1$ line at 5331.561 GHz has $E_{J=2} = 384.58 \text{ K}$ with $A_{21} = 5.16 \times 10^{-7} \text{ s}^{-1}$. The A-coefficients have been calculated using the dipole moment of $8.56 \times 10^{-4} \text{ D}$ ³³.

2. Simple Estimate of the Gas Mass

The mass implied by a line flux of optically thin emission from an unresolved source can be derived in two steps. The total number of HD molecules (\mathcal{N}_{HD}) is related to the line flux by this relation, assuming that the beam encompasses the source:

$$F_l = \frac{\mathcal{N}_{\text{HD}} A_{10} h \nu f_u}{4\pi D^2}. \quad (2)$$

In this expression $f_u = 3.0 * \exp(-128.5 \text{ K}/T)/Q(T)$ is the fractional of HD molecules in $J = 1$, D is the distance, and ν is the frequency. Converting to mass, and assuming all is in H₂, $M_{\text{gas disk}} = 2.37 * m_{\text{H}} \mathcal{N}_{\text{HD}}/x_{\text{HD}}$, where x_{HD} is the abundance of HD relative to H₂, m_{H} is the mass of a hydrogen atom, and 2.37 is the mean molecular weight per particle, including helium and heavy elements³⁴. This gives

$$M_{\text{gas disk}} = \frac{2.37 m_{\text{H}} 4\pi D^2 F_l}{A_{10} h \nu x_{\text{HD}} f_u}. \quad (3)$$

The partition function, $Q(T)$, is near unity below $\sim 50 \text{ K}$ ³². Inserting values of physical constants yields:

$$M_{gas\ disk} > 5.21 \times 10^{-5} \left(\frac{F_l}{6.3 \times 10^{-18} \text{ W m}^{-2}} \right) \left(\frac{3 \times 10^{-5}}{x_{HD}} \right) \left(\frac{D}{55 \text{ pc}} \right)^2 \exp \left(\frac{128.5 \text{ K}}{T_{gas}} \right) M_{\odot}. \quad (4)$$

This estimate represents a lower limit because the HD emission may not trace all the mass in the disk.

3. CO Emission and T_{gas} from TW Hya

In the main text we used the resolved ALMA Science Verification CO $J = 3 \rightarrow 2$ data to set a limit on the gas temperature. In Supplementary Figure 1 we show the integrated emission map with a beam size $1.7'' \times 1.5''$, which corresponds to a radius of 47×41 AU. The map demonstrates that the CO emission is resolved, so we assume unity filling factor. Based on the central spectrum the observed peak radiation temperature is $T_R = 22.2 \pm 0.1$ K (we note that this data has a calibration uncertainty of 10%). T_R is linearly related to the intensity, so a correction for the difference between the Planck function and the Rayleigh-Jeans approximation results in an average gas kinetic temperature of $T_{gas} = 29.7$ K in the beam, assuming optically thick and thermalized emission. Observations of CO $J = 6 \rightarrow 5$ confirm this value. The observed CO $J = 6 \rightarrow 5$ peak intensity is $T_R = 16.9 \pm 3.2$ K³⁵, which corresponds to a gas temperature of 30.6 K.

Assuming $T_{gas} = 30$ K yields a minimum disk mass of $3.9 \times 10^{-3} M_{\odot}$.

4. HD Emission Line Models

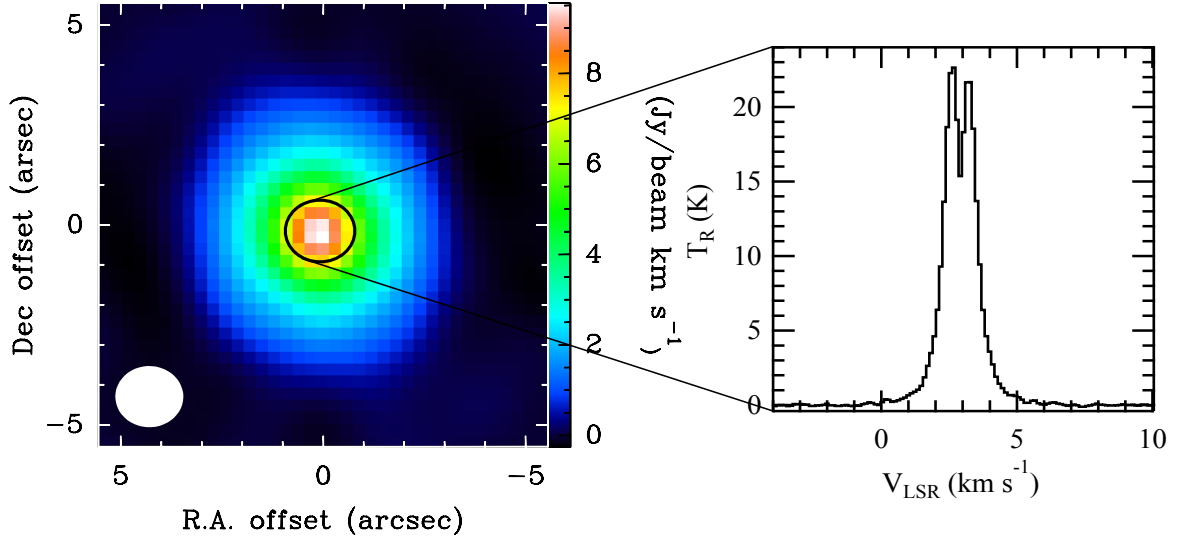
For more detailed models we use two predicted physical structures (Gorti et al.¹⁴ and the Thi et al.¹³ TW Hya models) derived from thermochemical calculations that match a range of gas phase emission lines. The Gorti et al. TW Hya model has a disk gas mass of $0.06 M_{\odot}$, and we used direct output from the model. For the Thi et al. TW Hya model we use a reproduction. Specifically, to reproduce this model we adopt the physical parameters for the dust structure as given in their¹³ Table 2. The dust optical constants are as prescribed³⁶ with a dust grain size distribution from $3 \times 10^{-2} \mu\text{m}$ to 1 mm and a power law index of 3.4. These inputs were placed into RADMC³⁷ where we verified that the model reproduced the observed spectral energy distribution and the dust thermal structure given in their Fig. A.2. For this calculation the total disk gas mass is $0.003 M_{\odot}$ and we verified that our gas density distribution matched that provided in their Figure A.1. We do not model the H-H₂ transition; this is appropriate for HD which will emit below this transition region. Finally we used the gas temperature distribution given in their Fig. A.3 as input to our LIME calculations for HD. As a final check we computed the predicted emission of this reproduction for CO and $^{13}\text{CO } J = 3 \rightarrow 2$ to observed values³⁸ and found them to be in agreement to within a factor of two.

To predict the HD line emission from the physical models we calculate the solution of the equations of statistical equilibrium including the effects of line and dust opacity using the LIME code³⁰. Although the HD line emission is fairly close to LTE, we adopt the collision rate coefficients of HD with H₂³⁹. The collision rates are insensitive to the rotational state of the H₂ collision partner⁴⁰. The disk dust optical depth is determined by the dust opacity coefficient κ_λ and the dust mass distribution within the disk. Typical dust mixtures^{36,41} suggest $\kappa_{112\ \mu m} \sim 30\ \text{cm}^2\ \text{g}^{-1}$. The excitation model explicitly explores pumping by continuum radiation, which is found to be negligible when compared to the effects of the dust optical depth. Table S1 provides the predictions from the specific thermochemical model including an emission calculation with dust opacity at $112\ \mu\text{m}$ (the realistic case) and without dust opacity. The Thi et al. TW Hya model with the lowest mass predicts an HD emission line that is too weak. To match observations within the framework of the Thi et al. TW Hya model we require an increase in mass by a factor of 20. We stress that this is approximate as scaling the mass will change the thermal solution (gas temperature, chemistry). Thus, this factor only illustrates the mass dependency and is not definitive. The thermochemical model that comes closest to the observed flux is the Gorti et al. TW Hya $0.06\ M_\odot$ model – which is still about a factor of two smaller than the observed HD emission.

Supplementary Table S1: Specific Model Predictions

Disk Model	Gas Mass	HD $J = 1 \rightarrow 0^a$	HD $J = 2 \rightarrow 1$
	(M_\odot)	(W m^{-2})	(W m^{-2})
Thi et al. TW Hya	0.003	3.8×10^{-19}	1.4×10^{-19}
Gorti et al. TW Hya	0.06	3.1×10^{-18}	3.3×10^{-18}
Observations		$6.3 \pm 0.7 \times 10^{-18}$	$< 8.0 \times 10^{-18}$

^aFluxes without dust optical depth are $7.4 \times 10^{-19}\ \text{W m}^{-2}$ (Thi et al. $0.003\ M_\odot$),
 $4.2 \times 10^{-18}\ \text{W m}^{-2}$ (Gorti et al. $0.06\ M_\odot$)



Supplementary Figure 3: ALMA Science Verification Observations of CO $J = 3 \rightarrow 2$ in TW Hydra. (Left) Map of CO $J = 3 \rightarrow 2$ integrated emission with intensity scale given on the left. The beam size of this observation is $1.7'' \times 1.5''$ and is shown in the figure. (Right) Blow-up of the central spectrum.